

**Probing quark gluon plasma properties by heavy flavors**Santosh K. Das, Jan-e Alam,<sup>\*</sup> and Payal Mohanty*Variable Energy Cyclotron Centre, 1/AF, Bidhan Nagar, Kolkata-700064, India*

(Received 3 September 2009; published 30 November 2009)

The Fokker-Planck (FP) equation has been solved to study the interaction of nonequilibrated heavy quarks with the quark gluon plasma expected to be formed in heavy ion collisions at Relativistic Heavy Ion Collider energies. Solutions of the FP equation have been convoluted with the relevant fragmentation functions to obtain the  $D$  and  $B$  meson spectra. Results are compared with experimental data measured by the STAR Collaboration. It is found that the present experimental data cannot distinguish  $p_T$  spectra obtained from the equilibrium versus the nonequilibrium charm distributions. Data at lower  $p_T$  may play a crucial role in making the distinction between the two. The nuclear suppression factor  $R_{AA}$  for nonphotonic single-electron spectra resulting from semileptonic decays of hadrons containing heavy flavors has been evaluated using the present formalism. It is observed that the experimental data on the nuclear suppression factor of nonphotonic electrons can be reproduced within this formalism by enhancing the perturbative QCD cross sections by a factor of 2, provided that the expansion of the bulk matter is governed by the velocity of sound  $c_s \sim 1/\sqrt{4}$ . The ideal-gas equation of state fails to reproduce the data even with enhancement of the perturbative QCD cross sections by a factor of 2.

DOI: [10.1103/PhysRevC.80.054916](https://doi.org/10.1103/PhysRevC.80.054916)

PACS number(s): 12.38.Mh, 24.85.+p, 25.75.Nq

**I. INTRODUCTION**

Nuclear collisions at Relativistic Heavy Ion Collider (RHIC) and Large Hadron Collider (LHC) energies are aimed at creating a phase of matter where the properties are governed by quarks and gluons [1]. This phase of matter, composed of mainly light quarks and gluons, is called quark gluon plasma (QGP). Study of the bulk properties of QGP is a field of great contemporary interest and the heavy flavors, namely, charm and bottom quarks, play a crucial role in such studies. Because they are produced in the early stage of collisions, they are not part of the bulk properties of the system and their thermalization time scale is longer than that of light quarks and gluons and, hence, can retain the interaction history more effectively.

The successes of the relativistic hydrodynamical model [2,3] in describing the host of experimental results from the RHIC [4] indicate that thermalization may have taken place in the system of quarks and gluons formed after nuclear collisions. The strong final-state interaction of high-energy partons with the QGP, that is, the observed jet quenching [5,6] and the large elliptic flow ( $v_2$ ) [7,8], in Au + Au collisions at RHIC energy indicate the possibility of fast equilibration. On the one hand, experimental data indicate an early thermalization time,  $\sim 0.6$  fm/c [9]; on the other hand, perturbative QCD (pQCD)-based calculations give a thermalization time of  $\sim 2.5$  fm/c [10] (see also Ref. [11]). The gap between these two time scales suggests that nonperturbative effects play a crucial role in achieving thermalization. It has also been pointed out that the instabilities [12–15] may drive the system toward faster equilibration. Two pertinent issues regarding equilibration are addressed here: (i) Do the heavy quarks achieve equilibrium? and (ii) If they do, can the equilibrium be maintained during expansion of the system? The second issue is addressed first.

We make the rather strong assumption that the heavy quarks produced initially are in thermal equilibrium and check whether they can maintain equilibrium during the entire evolution processes by comparing their scattering rates with the expansion rate of the matter. This issue is addressed with different equations of state (EOS), which affect the expansion rate. If the heavy quarks are unable to maintain equilibrium, then analysis of the transverse momentum of mesons carrying heavy flavors cannot be done using the thermal phase space distribution. The analysis will require nonequilibrium statistical mechanical treatment. We solve the Fokker-Planck (FP) equation [16–23] to address this issue, as discussed later.

The pQCD calculations indicate that the heavy quark thermalization time  $\tau_i^Q$  is longer [19] than that of the light quark and gluon thermalization scale  $\tau_i$ . Gluons may thermalize before up and down quarks [18,24]; in the present work we assume that the QGP is formed at time  $\tau_i$ . Therefore, the interaction of the nonequilibrated heavy quark ( $Q$ ) with the equilibrated QGP for the time interval  $\tau_i < \tau < \tau_i^Q$  can be treated within the ambit of the FP equation; that is, the heavy quark can be thought of as executing Brownian motion in the heat bath of QGP during the said interval of time. The solution of the FP equation can be used to study  $p_T$  spectra of heavy mesons in the spirit of the blast-wave method.

In the next section we address the issues of thermalization in a rapidly expanding system. The results indicate that heavy quarks cannot maintain equilibrium at RHIC and LHC energies during the entire evolutionary history of the QGP. This demands treatment of the problem within the framework of nonequilibrium statistical mechanics, which is discussed in Sec. III. Section IV is devoted to a summary and conclusions.

**II. THERMALIZATION IN AN EXPANDING SYSTEM**

We consider a thermally equilibrated partonic system of quarks, antiquarks, and gluons produced in relativistic heavy

<sup>\*</sup>[jane@veccal.ernet.in](mailto:jane@veccal.ernet.in)

ion collisions. We wish to study whether the system can maintain thermal equilibrium when it evolves in space and time. Relativistic hydrodynamics (with boost invariance along the longitudinal direction and cylindrical symmetry) have been used to describe the space-time evolution. For this purpose, the scattering time scale ( $\tau_{\text{scatt}}$ ) of the partons is compared with the expansion time scale ( $\tau_{\text{exp}}$ ). For maintenance of thermal equilibrium the following criterion should be satisfied:

$$\tau_{\text{exp}} \geq \alpha \tau_{\text{scatt}}, \quad (1)$$

where  $\alpha \sim O(1)$  is a constant. The criterion given in Eq. (2) is the reverse of the one used to study the freeze-out of various species of particles during the evolution of the early universe [25] (a similar condition is used in Ref. [26] for heavy ion collisions also).

The  $\tau_{\text{scatt}}$  is determined for each parton by the expression

$$\tau_{\text{scatt}}^i = \frac{1}{\sum \sigma_{ij} v_{ij} n_j}, \quad (2)$$

where  $\sigma_{ij}$  is the total cross section for particles  $i$  and  $j$ ,  $v_{ij}$  is the relative velocity between particle  $i$  and particle  $j$ , and  $n_j$  is the density of particle type  $j$ .

To calculate the scattering time we use the processes  $gg \rightarrow gg$ ,  $gg \rightarrow q\bar{q}$ ,  $q(\bar{q})g \rightarrow q(\bar{q})g$ ,  $qq \rightarrow qq$ , and  $q\bar{q} \rightarrow q\bar{q}$  for light flavors and gluons [27]. Here  $q$  stands for light quarks and  $g$  denotes gluons. For evaluating  $\tau_{\text{scatt}}$  for heavy quarks ( $Q$ ) the pQCD processes are taken from Ref. [28]. The infrared divergence appearing in the case of massless particle exchange in the  $t$  channel has been shielded by the Debye mass.

The expansion time scale can be defined as

$$\tau_{\text{exp}}^{-1} = \frac{1}{\epsilon(\tau, r)} \frac{d\epsilon(\tau, r)}{d\tau}, \quad (3)$$

where  $\epsilon(\tau, r)$  is the energy density, and  $\tau$  and  $r$  are the proper time and the radial coordinate, respectively.  $\epsilon(\tau, r)$  is calculated by solving the hydrodynamical equation:

$$\partial_\mu T^{\mu\nu} = 0, \quad (4)$$

with the assumption of boost invariance along the longitudinal direction [29] and cylindrical symmetry of the system [30]. In Eq. (4),  $T^{\mu\nu} = (\epsilon + P)u^\mu u^\nu - g^{\mu\nu}P$  is the energy momentum tensor,  $P$  is the pressure,  $u^\mu$  denotes the four-velocity, and  $g^{\mu\nu}$  is the metric tensor. We consider a net baryon-free QGP here; therefore the baryonic chemical potential ( $\mu_B$ ) is zero.

Expansion rates for RHIC and LHC energies were calculated using the initial conditions  $T_i = 400$  MeV and  $\tau_i = 0.2$  fm for RHIC, which gives  $dN/dy \sim 1100$  [4], and  $T_i = 700$  MeV and  $\tau_i = 0.08$  fm for LHC, giving  $dN/dy = 2100$  [31]. The initial radial velocity was taken as zero for both cases. Two sets (Sets I and II) of EOS were used to study the sensitivity of the results to the EOS.

In Set I, in a first-order phase transition scenario, we use the bag model EOS for the QGP phase and consider all resonances with mass  $\leq 2.5$  GeV for the hadronic phase [32]. In Set II the EOS is taken from lattice QCD calculations performed by the MILC Collaboration [33].

In Fig. 1 the scattering time scale is contrasted with the expansion time scale for the two types of EOS just mentioned.

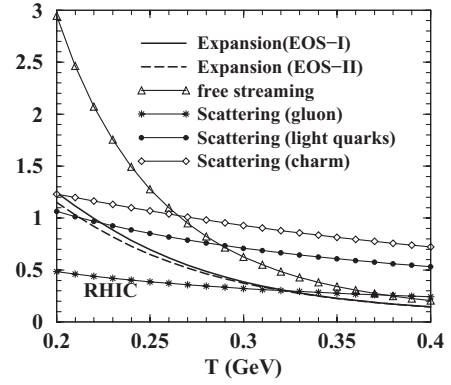


FIG. 1. Expansion time vs scattering time (calculated with the pQCD process) at RHIC energy. Here the expansion time scale was calculated at  $r = 1$  fm.

For the sake of comparison the expansion rate for the extreme case of free streaming is also displayed. Scattering rates are evaluated with pQCD cross sections. The condition for equilibration in Eq. (1) indicates that the gluons remain close to equilibrium; however, the charm and bottom (not shown in the figure) quarks remain out of equilibrium during the entire evolution history.

However, as mentioned in Sec. I, analysis of the experimental data within the ambit of relativistic hydrodynamics suggests that the matter formed in Au + Au collisions at the RHIC achieve thermalization. One possible cause of this thermalization is that the partons interact strongly after their formation in heavy ion collisions. It is argued in Ref. [34] that the onset of thermalization in systems formed in heavy ion collisions at relativistic energies cannot be achieved without nonperturbative effects. It has also been shown, in Ref. [35], that a large enhancement of the pQCD cross section is required for reproduction of experimental data on elliptic flow at RHIC energies. Therefore, the pQCD cross sections used to derive the results shown in Fig. 1 should include nonperturbative effects. To implement this we enhanced the pQCD cross sections by a factor of 2. The resulting scattering time is compared with the expansion time in Fig. 2. It is observed that gluons are kept in equilibrium throughout the evolution, and light quarks are closer to equilibrium compared to the heavy flavors.

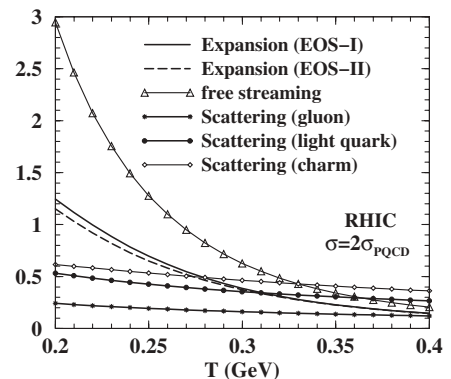


FIG. 2. Same as Fig. 1, with the pQCD cross section enhanced by a factor of 2.

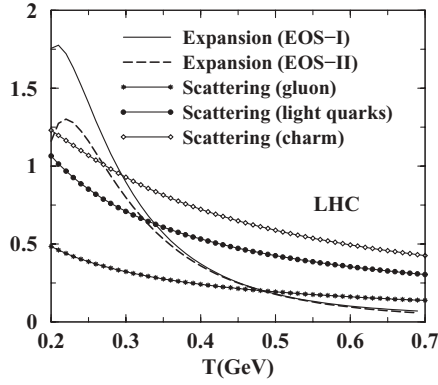


FIG. 3. Same as Fig. 1, for LHC energy.

In Figs. 3 and 4 the results for LHC are displayed for the two time scales mentioned previously for pQCD and enhanced cross sections. Expansion becomes faster at LHC than at RHIC energies because of the higher internal pressure. As a consequence, it is interesting to note that the thermalization scenario at LHC energy does not differ drastically from that at RHIC energy.

### III. NONEQUILIBRIUM PROCESS

It is argued in Ref. [19] that the relaxation time for heavy quarks is longer than that for light partons by a factor of  $M/T$ , where  $M$  is the mass of the heavy flavor and  $T$  is the temperature. In the present work we have also seen that heavy flavors do not maintain equilibration throughout the evolutionary scenario, but gluons are close to equilibrium. Therefore, we treat this problem as an interaction between equilibrium and nonequilibrium degrees of freedom, and the FP equation provides an appropriate framework for such studies.

The Boltzmann transport equation describing a nonequilibrium statistical system reads

$$\left( \frac{\partial}{\partial t} + \frac{p}{E} \frac{\partial}{\partial x} + F \frac{\partial}{\partial p} \right) f(x, p, t) = \left( \frac{\partial f}{\partial t} \right)_{\text{col}}. \quad (5)$$

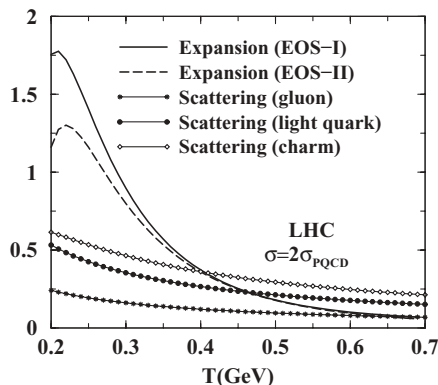


FIG. 4. Same as Fig. 2, for LHC energy.

The assumption of uniformity in the plasma and absence of any external force leads to

$$\frac{\partial f}{\partial t} = \left( \frac{\partial f}{\partial t} \right)_{\text{col}}. \quad (6)$$

The collision term on the right-hand side of Eq. (6) can be approximated as (see Refs. [17] and [36] for details)

$$\left( \frac{\partial f}{\partial t} \right)_{\text{col}} = \frac{\partial}{\partial p_i} \left\{ A_i(p) f + \frac{\partial}{\partial p_i} [B_{ij}(p) f] \right\}, \quad (7)$$

where we have defined the kernels

$$A_i = \int d^3 p \omega(p, k) k_i, \quad (8)$$

$$B_{ij} = \int d^3 p \omega(p, k) k_i k_j,$$

and the function  $\omega(p, k)$  is given by

$$\omega(p, k) = g_j \int \frac{d^3 q}{(2\pi)^3} f_j(q) v_{ij} \sigma_{p, q \rightarrow p-k, q+k}^j, \quad (9)$$

where  $f_j$  is the phase space distribution for particle  $j$ ,  $v_{ij}$  is the relative velocity between the two collision partners,  $\sigma$  denotes the cross section, and  $g_j$  is the statistical degeneracy. The coefficients in the first two terms of the expansion in Eq. (7) are comparable in magnitude because the averaging of  $k_i$  involves greater cancellation than the averaging of the quadratic term  $k_i k_j$ . The higher power of  $k_i$  values is smaller [37].

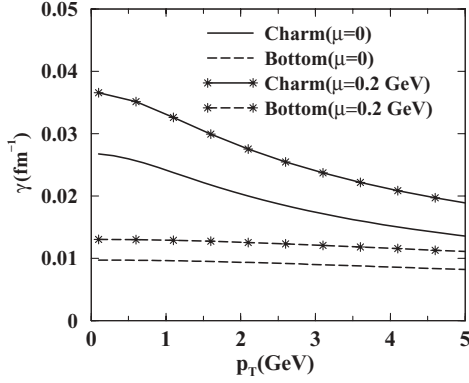
With these approximations the Boltzmann equation reduces to a nonlinear integro-differential equation known as the Landau kinetic equation:

$$\frac{\partial f}{\partial t} = \frac{\partial}{\partial p_i} \left\{ A_i(p) f + \frac{\partial}{\partial p_i} [B_{ij}(p) f] \right\}. \quad (10)$$

The nonlinearity is caused by the appearance of  $f$  in  $A_i$  and  $B_{ij}$  through  $w(p, k)$ . It arises from the simple fact that we are studying a collision process that involves two particles; it should, therefore, depend on the states of the two participating particles in the collision process and, hence, on the product of the two. Considerable simplicity may be achieved by replacing the distribution functions of the collision partners of the test particle by their equilibrium Fermi-Dirac or Bose-Einstein distributions (depending on the statistical nature) in the expressions of  $A_i$  and  $B_{ij}$ . Then Eq. (10) reduces to a linear partial differential equation—usually referred to as the FP equation [38]—describing the motion of a particle that is out of thermal equilibrium with the particles in a thermal bath. The quantities  $A_i$  and  $B_{ij}$  are related to the usual drag and diffusion coefficients and we denote them  $\gamma_i$  and  $D_{ij}$ , respectively (i.e., these quantities can be obtained from the expressions for  $A_i$  and  $B_{ij}$  by replacing the distribution functions with their thermal counterparts):

$$\frac{\partial f}{\partial t} = \frac{\partial}{\partial p_i} \left\{ \gamma_i(p) f + \frac{\partial}{\partial p_i} [D_{ij}(p) f] \right\}. \quad (11)$$

We evaluate the value of  $\gamma_i$  and  $D_{ij}$  for the reactions  $gQ \rightarrow gQ$  and  $qQ \rightarrow qQ$  for both zero and nonzero quark chemical potentials ( $\mu = \mu_B/3$ ). In Fig. 5 we depict the variation of the drag coefficients as a function of the transverse momentum of

FIG. 5. Variation of drag coefficient with  $p_T$  for  $T = 200$  MeV.

the charm and bottom quarks at a temperature  $T = 200$  MeV. The momentum dependence is weak. For nonzero quark chemical potential the value of the drag increases; however, the nature of the variations remains the same. In Fig. 6 the temperature variation of the drag coefficient is plotted for both zero and nonzero quark chemical potentials. Qualitatively, the inverse of the drag coefficient gives the magnitude of the relaxation time. Therefore, the present results indicate that a system with a fixed temperature achieves equilibrium faster for nonzero  $\mu$ . In Fig. 7 the diffusion coefficients are plotted as a function of  $p_T$  for  $T = 200$  MeV. The diffusion coefficient for nonzero  $\mu$  is higher compared to the case of vanishing  $\mu$ . The same quantity is displayed in Fig. 8 as a function of temperature. In the present work we confine  $\mu = 0$ . Recently the heavy quark momentum diffusion coefficient has been computed [39] at next to leading order within the the ambit of hard thermal loop approximations. For  $T \sim 400$  MeV our momentum-averaged pQCD value of the diffusion coefficient is comparable to the value obtained in Ref. [39] in the leading order approximation for the same set of inputs (e.g., strong coupling constant and same number of flavors).

The inverse of the drag coefficient gives an estimate of the thermalization time scale. Results obtained in the present work indicate that heavy quarks are unlikely to attain thermalization at RHIC and LHC energies [40].

The total amount of energy dissipated by a parton depends on the path length it traverses through the plasma. Each

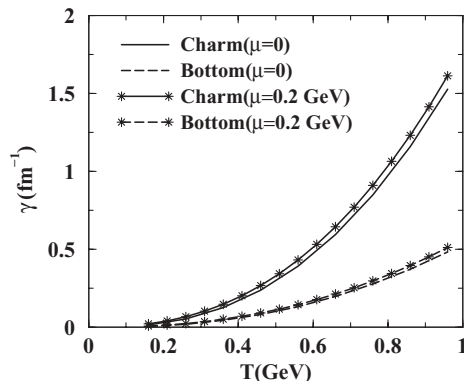
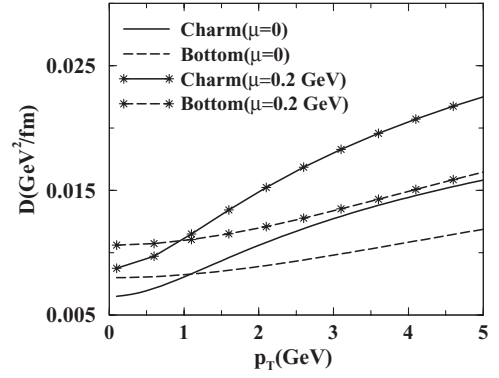


FIG. 6. Variation of drag coefficient with temperature.

FIG. 7. Variation of diffusion coefficient with  $p_T$  for  $T = 200$  MeV.

parton traverses a different path length, which depends on the geometry of the system and on the point where it is produced. The probability that a parton is created at a point  $(r, \phi)$  in the plasma depends on the number of binary collisions at that point, which can be taken as [21]

$$P(r, \phi) = \frac{2}{\pi R^2} \left(1 - \frac{r^2}{R^2}\right) \theta(R - r), \quad (12)$$

where  $R$  is the nuclear radius. A parton created at  $(r, \phi)$  in the transverse plane propagates a distance  $L = \sqrt{R^2 - r^2 \sin^2 \phi} - r \cos \phi$  in the medium. In the present work we adopt the following averaging procedure for transport coefficients. For the drag coefficient ( $\gamma$ ),

$$\Gamma = \int r dr d\phi P(r, \phi) \int^{L/v} d\tau \gamma(\tau), \quad (13)$$

where  $v$  is the velocity of the propagating partons. The quantity  $\Gamma$  appears in the solution of the FP equation (see Ref. [20] for details). Similar averaging has been done for the expression involving diffusion coefficients to take into account the geometry of the system.

Using the drag and diffusion coefficients as inputs we solve the FP equation with the following parametrization of the initial momentum distribution of the charm quarks generated

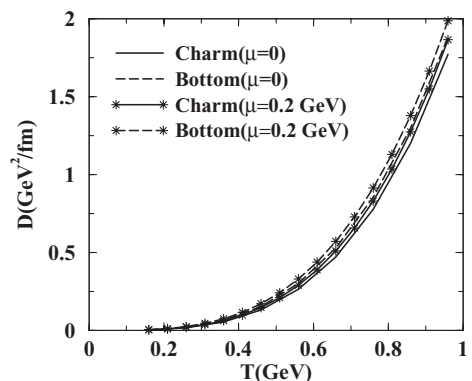


FIG. 8. Variation of diffusion coefficient with temperature.



in  $p$ - $p$  collisions at  $\sqrt{s} = 200$  GeV:

$$\frac{d^2 N_c}{dp_T^2} = C \frac{(p_T + A)^2}{[1 + (p_T/B)]^\alpha}, \quad (14)$$

where  $A = 0.5$  GeV,  $B = 6.6$  GeV,  $\alpha = 21$ , and  $C = 0.845$  GeV $^{-4}$ . We do not elaborate here on the procedure for solving the FP equation, as this is discussed in detail in Ref. [20]. The corresponding initial distributions for bottom quarks can be obtained from the results obtained in Ref. [41] for  $p$ - $p$  collisions at  $\sqrt{s} = 200$  GeV. Obtaining the solution of the FP equation for heavy (charm and bottom) quarks, we convolute it with the fragmentation functions of the heavy quarks to obtain the  $p_T$  distribution of the  $D$  and  $B$  mesons. The following three sets of fragmentation functions were used to check the sensitivity of the results.

In Set I [42]

$$f(z) \propto \frac{1}{z^{1+r_Q b m_Q^2}} (1-z)^a \exp\left(-\frac{b m_T^2}{z}\right), \quad (15)$$

where  $m_Q$  is the mass of the charm quark,  $r_Q = 1$ ,  $a = 5$ ,  $b = 1$ , and  $m_T^2 = m_Q^2 + p_T^2$ . It has been explicitly checked that  $R_{AA}$  is not very sensitive to the values of  $a$  and  $b$ .

In Set II [43]

$$f(z) \propto z^\alpha (1-z), \quad (16)$$

where  $\alpha = -1$  for the charm quark and 9 for the bottom quark.

In Set III [44]

$$f(z) \propto \frac{1}{z \left(z - \frac{1}{z} - \frac{\epsilon_c}{1-z}\right)^2}, \quad (17)$$

where for the charm quark  $\epsilon_c = 0.05$  and for the bottom quark  $\epsilon_b = (m_c/m_b)^2 \epsilon_c$ .

Recently, the  $p_T$  spectrum of  $D$  mesons has been measured by the STAR Collaboration [45] in Au + Au collisions at  $\sqrt{s_{NN}} = 200$  GeV. The  $p_T$  spectrum of hadrons can be written as [46]

$$\frac{dN}{d^2 p_T dy} = \frac{g}{(2\pi)^3} \int \tau r d\phi d\eta [m_T \cosh(\eta - y) - p_T \cos\phi d\tau] f(u^\mu p_\mu), \quad (18)$$

where  $\eta$  is the space-time rapidity,  $p^\mu$  is the four-momentum,  $u^\mu = \gamma(1, \beta)$  is the hydrodynamic four-velocity,  $u^\mu p_\mu$  is the energy of the hadrons in the comoving frame of the plasma, and  $f(u^\mu p_\mu)$  is the momentum space distribution. In the spirit of the blast-wave method we can write Eq. (18) as [47]

$$\frac{dN}{d^2 p_T dy} = \frac{g}{(2\pi)^3} \int \tau r d\phi d\eta m_T \cosh(\eta - y) f(u^\mu p_\mu) dr. \quad (19)$$

Taking the surface velocity profile as

$$\beta(r) = \beta_s \left(\frac{r}{R}\right)^n, \quad (20)$$

and choosing  $n = 1$ , once can evaluate  $p_T$  spectrum of  $D$  mesons.

Before comparing the data with the nonequilibrium momentum distribution, we analyze the data within the ambit of

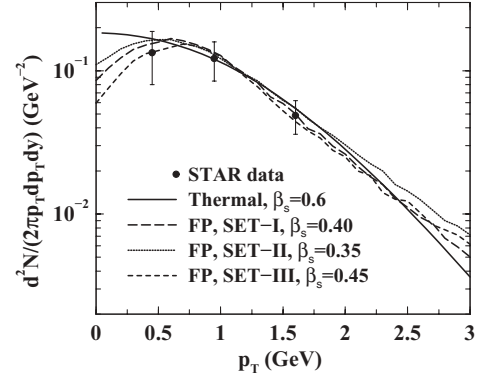


FIG. 9. Invariant momentum distribution of the  $D$  meson as a function of  $p_T$ .

the blast-wave method [47] assuming an equilibrium distribution for the  $D$  meson. The values of the blast-wave parameters, that is, the radial flow velocity at the surface  $\beta_s$  and the freeze-out temperature  $T_F$ , are 0.6 and 0.170 GeV, respectively. The data are reproduced well (Fig. 9). The value of  $T_F$  is close to  $T_c$ , which indicates that the  $D$  mesons (even if the charm is in equilibrium in the partonic phase) cannot maintain equilibrium in the hadronic phase. This is reasonable because of the low interaction cross sections of the  $D$  mesons with other hadrons. Next we replace the equilibrium distribution in Eq. (19) with the solution of the FP equation appropriately boosted by the radial velocity. The results are displayed in Fig. 9. The data are reproduced well for all three sets of fragmentation functions mentioned before. The value of the freeze-out temperature is 170 MeV and the flow velocity at the surface is 0.45, 0.35, and 0.4 for the Set I, Set II, and Set III fragmentation functions, respectively. The value of  $\beta_s$  is lower here than in the equilibrium case for all fragmentation functions. It is interesting to note that in a low- $p_T$  ( $\leq 0.5$ -GeV) domain the results for the equilibrium distribution differ substantially from those for the nonequilibrium distribution for all three sets of fragmentation functions. Therefore, measurements of the heavy meson spectra in a low- $p_T$  domain will be very useful to distinguish between the equilibrium and the nonequilibrium scenarios. The two scenarios also give different kinds of variation at high  $p_T$ . The  $p_T$ -integrated quantity, that is, the  $D$ -meson multiplicity, may also be useful to understand the difference between the equilibrium and the nonequilibrium scenarios.

#### IV. NONPHOTONIC SINGLE ELECTRON FROM HEAVY FLAVORS

The STAR [48] and PHENIX [49] Collaborations have recently measured nonphotonic single-electron inclusive  $p_T$  spectra for both Au + Au and  $p + p$  collisions at  $\sqrt{s_{NN}} = 200$  GeV. The quantity

$$R_{AA}(p_T) = \frac{\left(\frac{dN^e}{d^2 p_T dy}\right)^{\text{Au+Au}}}{N_{\text{coll}} \left(\frac{dN^e}{d^2 p_T dy}\right)^{p+p}}, \quad (21)$$

called the nuclear suppression factor, will be unity in the absence of any medium. However, the experimental data from both collaborations [48,49] show substantial suppression ( $R_{AA} < 1$ ) for  $p_T \geq 2$  GeV, indicating the interaction of the plasma particles with the charm and bottom quarks from which electrons are originated through the process  $c(b)$  (hadronization)  $\rightarrow D(B)$  (decay)  $\rightarrow e + X$ . The loss of energy of high- $p_T$  heavy quarks propagating through the medium created in Au + Au collisions causes a depletion of high- $p_T$  electrons.

To evaluate  $R_{AA}$  theoretically, the solution of the FP equation for the charm and bottom quarks should be convoluted by the fragmentation functions to obtain the  $p_T$  distribution of the  $D$  and  $B$  mesons, which subsequently decay through the processes  $D \rightarrow Xev$  and  $B \rightarrow Xev$ . Similar formalism has been used in Ref. [50] to study the evolution of light quark momentum distributions. The resulting electron spectra from the decays of  $D$  and  $B$  mesons can be obtained as follows [51–53]:

$$\frac{dN^e}{p_T dp_T} = \int dq_T \frac{dN^D}{q_T dq_T} F(p_T, q_T), \quad (22)$$

where

$$F(p_T, q_T) = \omega \int \frac{d(\mathbf{p}_T \cdot \mathbf{q}_T)}{2p_T(\mathbf{p}_T \cdot \mathbf{q}_T)} g[(\mathbf{p}_T \cdot \mathbf{q}_T)/M], \quad (23)$$

where  $M$  is the mass of the heavy mesons ( $D$  or  $B$ ),  $\omega = 96(1 - 8m^2 + 8m^6 - m^8 - 12m^4 \ln m^2)^{-1} M^{-6}$  ( $m = m_X/M$ ), and  $g(E_e)$  is given by

$$g(E_e) = \frac{E_e^2(M^2 - M_X^2 - 2ME_e)^2}{(M - 2E_e)}, \quad (24)$$

related to the rest frame spectrum for the decay  $D(B) \rightarrow Xev$  by the following relation [51]:

$$\frac{1}{\Gamma} \frac{d\Gamma}{dE_e} = \omega g(E_e). \quad (25)$$

We evaluate the electron spectra from the decays of heavy mesons originating from the fragmentation of heavy quarks propagating through the QGP medium formed in heavy ion collisions. Similarly the electron spectrum from  $p$ - $p$  collisions can be obtained from the charm and bottom quark distributions, which goes as initial conditions to the solution of the FP equation. The ratio of these two quantities gives the nuclear suppression  $R_{AA}$ . For a static system the temperature dependence of the drag and diffusion coefficients of heavy quarks enters via the thermal distributions of light quarks and gluons through which it is propagating. However, in the present scenario the variation of temperature with time is governed by the EOS or velocity of sound of the thermalized system undergoing hydrodynamic expansion. In such a situation quantities like  $\Gamma$  [Eq. (13)] and hence  $R_{AA}$  become sensitive to the velocity of sound in the medium.

The results for  $R_{AA}$  are displayed in Fig. 10. Theoretical results are obtained for the fragmentation function of Set I [42]. The velocity of sound for the QGP phase is taken as  $c_s = 1/\sqrt{4}$ , corresponding to the EOS  $P = \epsilon/4$ . The results fail to describe the data in this case. Next we generate  $R_{AA}$  by changing the value of  $c_s$  to  $1/\sqrt{5}$  and keeping all other

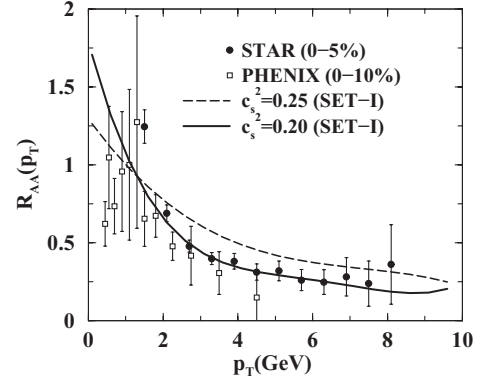


FIG. 10. Nuclear suppression factor  $R_{AA}$  as a function of  $p_T$ .

parameters fixed. The resulting spectrum describes the data reasonably well. A lower value of  $c_s$  makes the expansion of the plasma slower, enabling the propagating heavy quarks to spend more time interacting in the medium and hence lose more energy before exiting from the plasma, which results in less particle production at high  $p_T$ . Further lowering of  $c_s$  gives further suppression.

However, as mentioned earlier nonperturbative effects are important for the interaction of heavy quarks with the plasma. Therefore, we enhance the cross section by a factor of 2 and find that the experimental results can also be explained by taking the EOS  $P = \epsilon/4$  (Fig. 11) and keeping other quantities, such as fragmentation functions and so on, unchanged. The ideal-gas EOS  $P = \epsilon/3$  cannot reproduce the data even if the cross section is enhanced by a factor of 2. With  $c_s = 1/4$  and an enhanced cross section (by a factor of 2) the data can also be described for fragmentation functions of Sets II and III (Fig. 12). Several mechanisms, such as inclusions of nonperturbative contributions from the quasihadronic bound state [54], three-body scattering effects [55], and employment of running coupling constants and a realistic Debye mass [56], have been proposed to improve the description of the experimental data. It is demonstrated here that the EOS of the medium and nonperturbative effects play a crucial role in determining the nuclear suppression factor.

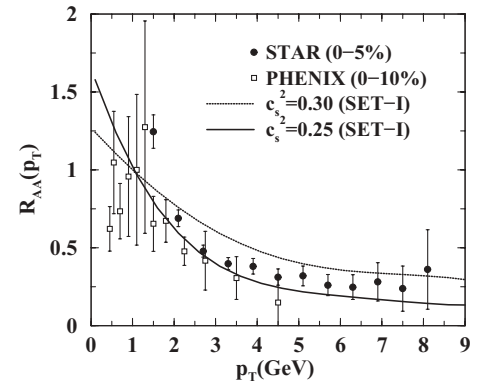


FIG. 11. Same as Fig. 10, with enhancement of the cross section by a factor of 2.

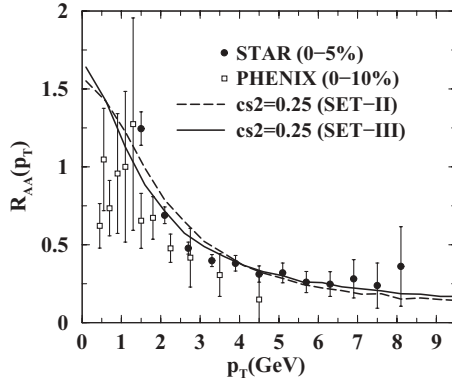


FIG. 12. Same as Fig. 11, for fragmentation functions of Sets II and III.

## V. SUMMARY AND CONCLUSIONS

The transverse momentum spectra of  $D$  and  $B$  mesons have been studied within the ambit of the FP equation where the charm and bottom quarks are executing Brownian motion in the heat bath of light quarks and gluons. We have evaluated the drag and diffusion coefficients for both zero and nonzero quark chemical potentials. Results for nonzero baryonic chemical potentials will be very useful for studying physics in low-energy RHIC runs [57]. Results have been compared with experimental data measured by the STAR Collaboration. It is found that the present experimental data cannot distinguish the  $p_T$  spectra obtained from equilibrium versus nonequilibrium charm distributions. Data at lower  $p_T$  may play a crucial role in making the distinction between the two. Because the results for equilibrium and nonequilibrium scenarios differ, the  $p_T$ -integrated quantity, that is, the  $D$ -meson multiplicity, may also be very useful for putting constraints on the model. The nuclear suppression factors for the measured nonphotonic single-electron spectra resulting from semileptonic decays of hadrons containing heavy flavors have been evaluated using the present formalism. The experimental data on nuclear suppression factors of nonphotonic electrons can be reproduced within this formalism if the expansion of the bulk matter is governed by the EOS  $P = \epsilon/4$  and the partonic cross sections are taken as  $2 \times \sigma_{\text{pQCD}}$ . Three kinds of fragmentation functions for the

charm and bottom quarks hadronizing to  $D$  and  $B$  mesons, respectively, have been used, and it is found that  $c_s \sim 1/\sqrt{4}$  can describe the data reasonably well. The data cannot be reproduced with  $c_s \sim 1/\sqrt{3}$ , even after enhancing the cross section by a factor of 2. The loss of energy by heavy quarks owing to the radiative process may be suppressed because of dead-cone effects. In the present work the radiative loss is neglected. The FP equation needs to be modified to include the radiative loss [58–62] (see Ref. [63] for a review); work in this direction is in progress [57].

The calculations may be improved by making the space-time evolutionary picture more rigorous as follows. In the absence of any external force the evolution of the heavy-quark phase-space distribution is governed by the equation

$$\left( \frac{\partial}{\partial t} + \mathbf{v}_p \cdot \nabla_{\mathbf{r}} \right) f(\mathbf{p}, \mathbf{r}, t) = C[f(\mathbf{p}, \mathbf{r}, t)]. \quad (26)$$

As mentioned before, the FP equation can be obtained from this equation by linearizing the collision term  $C[f(\mathbf{p}, \mathbf{r}, t)]$ . To take into account the energy loss of the heavy quarks in the thermal bath, the ideal hydrodynamic equation needs to be modified as

$$\partial_\mu T^{\mu\nu} = J^\nu, \quad (27)$$

containing the source term  $J^\nu$  corresponding to the energy momentum deposited in the thermal system along the trajectory of the heavy quark, which may be taken as  $J^\nu \sim dp^\nu/d\tau$  [64] (where  $p^\nu$  is the four-momentum vector). Equation (27) should be solved for  $T(\mathbf{r}, t)$  with the appropriate EOS, which can be used to obtain the surface of hadronization by setting  $T(\mathbf{r}_c, t_c) = T_c$ . Subsequently, the solution of Eq. (26),  $f(\mathbf{r}_c, t_c)$ , for the heavy quark on this surface should be convoluted with the fragmentation function to obtain the  $B$  and  $D$  distributions.

## ACKNOWLEDGMENTS

We are grateful to Bedanga Mohanty and Matteo Cacciari for very useful discussions. We also thank Jajati K. Nayak for his involvement in this work initially. The work was supported by DAE-BRNS Project Sanction No. 2005/21/5-BRNS/2455.

- 
- [1] J. Alam, S. Chattopadhyay, T. Nayak, B. Sinha, and Y. P. Viyogi (eds.), *J. Phys. G* **35** (2008) (Proc. Quark Matter 2008).
  - [2] P. Huovinen and P. V. Ruuskanen, *Annu. Rev. Nucl. Part. Sci.* **56**, 163 (2006).
  - [3] D. A. Teaney, arXiv:0905.2433 [nucl-th].
  - [4] I. Arsene *et al.* (BRAHMS Collaboration), *Nucl. Phys.* **A757**, 1 (2005); B. B. Back *et al.* (PHOBOS Collaboration), *ibid.* **A757**, 28 (2005); J. Adams *et al.* (STAR Collaboration), *ibid.* **A757**, 102 (2005); K. Adcox *et al.* (PHENIX Collaboration), *ibid.* **A757**, 184 (2005).
  - [5] S. S. Adler *et al.* (PHENIX Collaboration), *Phys. Rev. Lett.* **96**, 202301 (2006).
  - [6] J. Adams *et al.* (STAR Collaboration), *Phys. Rev. Lett.* **91**, 072304 (2003).
  - [7] S. S. Adler *et al.* (PHENIX Collaboration), *Phys. Rev. Lett.* **91**, 182301 (2003).
  - [8] K. H. Ackemann *et al.* (STAR Collaboration), *Phys. Rev. Lett.* **86**, 402 (2001).
  - [9] P. Arnold, J. Lenaghan, G. D. Moore, and L. G. Yaffe, *Phys. Rev. Lett.* **94**, 072302 (2005).
  - [10] R. Baier, A. H. Mueller, D. Schiff, and D. T. Son, *Phys. Lett.* **B539**, 46 (2002).
  - [11] P. Romatschke and R. Venugopalan, *Phys. Rev. Lett.* **96**, 062302 (2006).
  - [12] S. Mrowczynski, *Phys. Lett.* **B314**, 118 (1993); *Phys. Rev. C* **49**, 2191 (1994); *Phys. Lett.* **B393**, 26 (1997).
  - [13] P. Romatschke and M. Strickland, *Phys. Rev. D* **68**, 036004 (2003).

- [14] P. Arnold, J. Lenaghan, and G. D. Moore, *J. High Energy Phys.* **08** (2003) 002.
- [15] P. Arnold, G. D. Moore, and L. G. Yaffe, *J. High Energy Phys.* **01** (2003) 030.
- [16] S. Chakraborty and D. Syam, *Lett. Nuovo Cimento* **41**, 381 (1984).
- [17] B. Svetitsky, *Phys. Rev. D* **37**, 2484 (1988).
- [18] J. Alam, S. Raha, and B. Sinha, *Phys. Rev. Lett.* **73**, 1895 (1994).
- [19] G. D. Moore and D. Teaney, *Phys. Rev. C* **71**, 064904 (2005).
- [20] H. van Hees and R. Rapp, *Phys. Rev. C* **71**, 034907 (2005).
- [21] S. Turbide, C. Gale, S. Jeon, and G. D. Moore, *Phys. Rev. C* **72**, 014906 (2005).
- [22] J. Bjorker and R. Venugopalan, *Phys. Rev. C* **63**, 024609 (2001).
- [23] M. G. Mustafa and M. H. Thoma, *Acta Phys. Hung. A* **22**, 93 (2005).
- [24] E. Shuryak, *Phys. Rev. Lett.* **68**, 3270 (1992).
- [25] E. W. Kolb and M. S. Turner, *The Early Universe* (Addison-Wesley, New York, 1990).
- [26] F. S. Navarra, M. C. Nemes, U. Ornik, and S. Paiva, *Phys. Rev. C* **45**, R2552 (1992).
- [27] R. D. Field, *Application of Perturbative QCD* (Addison-Wesley, New York, 1989).
- [28] B. L. Combridge, *Nucl. Phys.* **B151**, 429 (1979).
- [29] J. D. Bjorken, *Phys. Rev. D* **27**, 140 (1983).
- [30] H. von Gersdorff, L. D. McLerran, M. Kataja, and P. V. Ruuskanen, *Phys. Rev. D* **34**, 794 (1986).
- [31] N. Armesto *et al.*, *J. Phys. G* **35**, 054001 (2008).
- [32] B. Mohanty and J. Alam, *Phys. Rev. C* **68**, 064903 (2003).
- [33] C. Bernard, T. Burch, C. E. DeTar, S. Gottlieb, L. Levkova, U. M. Heller, J. E. Hetrick, R. Sugar, and D. Toussaint, *Phys. Rev. D* **75**, 094505 (2007).
- [34] Y. V. Kovchegov, *Nucl. Phys.* **A762**, 298 (2005).
- [35] D. Molnar and M. Gyulassy, *Nucl. Phys.* **A697**, 495 (2002).
- [36] P. Roy, J. Alam, S. Sarkar, B. Sinha, and S. Raha, *Nucl. Phys.* **A624**, 687 (1997).
- [37] E. M. Lifshitz and L. P. Pitaevskii, *Physical Kinetics* (Butterworths-Heinemann, Oxford, 1981).
- [38] R. Balescu, *Equilibrium and Non-Equilibrium Statistical Mechanics* (Wiley, New York, 1975).
- [39] S. Caron-Huot and G. D. Moore, *J. High Energy Phys.* **02** (2008) 081; S. Caron-Huot and G. D. Moore, *Phys. Rev. Lett.* **100**, 052301 (2008).
- [40] M. G. Mustafa, D. Pal, and D. K. Srivastava, *Phys. Rev. C* **57**, 889 (1998).
- [41] M. Cacciari, P. Nason, and R. Vogt, *Phys. Rev. Lett.* **95**, 122001 (2005).
- [42] M. G. Bowler, *Z. Phys. C* **11**, 169 (1981).
- [43] V. G. Kartvelishvili, A. K. Likhoded, and V. A. Petrov, *Phys. Lett.* **B78**, 615 (1978).
- [44] C. Peterson, D. Schlatter, I. Schmitt, and P. M. Zerwas, *Phys. Rev. D* **27**, 105 (1983).
- [45] B. I. Abelev *et al.*, arXiv:0805.0364 [nucl-ex].
- [46] P. V. Ruuskanen, *Acta Phys. Pol. B* **18**, 551 (1986).
- [47] E. Schnedermann, J. Sollfrank, and U. Heinz, *Phys. Rev. C* **48**, 2462 (1993).
- [48] B. I. Abelev *et al.* (STAR Collaboration), *Phys. Rev. Lett.* **98**, 192301 (2007).
- [49] S. S. Adler *et al.* (PHENIX Collaboration), *Phys. Rev. Lett.* **96**, 032301 (2006).
- [50] P. Roy, A. K. Dutt-Mazumder, and J. Alam, *Phys. Rev. C* **73**, 044911 (2006).
- [51] M. Gronau, C. H. Llewellyn Smith, T. F. Walsh, S. Wolfram, and T. C. Yang, *Nucl. Phys.* **B123**, 47 (1977).
- [52] A. Ali, *Z. Phys. C* **1**, 25 (1979).
- [53] A. Chaudhuri, nucl-th/0509046.
- [54] H. van Hees, M. Mannarelli, V. Greco, and R. Rapp, *Phys. Rev. Lett.* **100**, 192301 (2008).
- [55] C. M. Ko and W. Liu, *Nucl. Phys.* **A783**, 233 (2007).
- [56] P. B. Gossiaux and J. Aichelin, *Phys. Rev. C* **78**, 014904 (2008).
- [57] S. K. Das *et al.*, in preparation.
- [58] A. Dainese, C. Loizides, and G. Paic, *Eur. Phys. J. C* **38**, 461 (2005); C. Loizides, *ibid.* **49**, 339 (2007).
- [59] M. Gyulassy, P. Levai, and I. Vitev, *Nucl. Phys.* **B571**, 197 (2000); M. Gyulassy, P. Levai, and I. Vitev, *Phys. Rev. Lett.* **85**, 5535 (2000); M. Gyulassy and X.-N. Wang, *Nucl. Phys.* **B420**, 583 (1994).
- [60] H. Zhang, J. F. Owens, E. Wang, and X. N. Wang, *Phys. Rev. Lett.* **98**, 212301 (2007).
- [61] R. Baier, Y. L. Dokshitzer, S. Peigne, and D. Schiff, *Phys. Lett.* **B345**, 277 (1995); R. Baier, Y. L. Dokshitzer, A. H. Mueller, and D. Schiff, *Nucl. Phys.* **B531**, 403 (1998).
- [62] C. A. Salgado and U. A. Wiedemann, *Phys. Rev. Lett.* **89**, 092303 (2002).
- [63] P. Jacobs and X. N. Wang, *Prog. Part. Nucl. Phys.* **54**, 443 (2005); R. Baier, D. Schiff, and B. G. Zakharov, *Annu. Rev. Nucl. Part. Sci.* **50**, 37 (2000).
- [64] A. K. Chaudhuri and U. Heinz, *Phys. Rev. Lett.* **97**, 062301 (2006); B. Betz, M. Gyulassy, D. H. Rischke, H. Stoecker, and G. Torrieri, *J. Phys. G* **35**, 104106 (2008).